MSX Force Field and Vibrational Frequencies for BEDT-TTF (Neutral and Cation)

Ersan Demiralp, Siddharth Dasgupta, and William A. Goddard III*

Materials and Process Simulation Center, Beckman Institute (139-74), Division of Chemistry and Chemical Engineering, California Institute of Technology, Pasadena, California 91125

Received: September 30, 1996; In Final Form: December 30, 1996[⊗]

BEDT-TTF is the donor of the highest T_c organic superconductors. Isotopic shift experiments support an electron−phonon coupling mechanism for the superconductivity. However, the vibrational levels have been only partially observed and assigned, making testing of this mechanism difficult. In order to provide a complete consistent description of all vibrational levels, we carried out Hartree−Fock calculations (6-31G** basis set) to obtain the Hessians and fundamental vibrational frequencies of BEDT-TTF and BEDT-TTF$^+$. With these Hessians and available experimental frequencies, we used Hessian-biased methods to develop the MSX force fields for the neutral and cation BEDT-TTF molecules. Comparison of the calculated frequencies with the available experimental frequencies for the neutral and cation BEDT-TTF molecule shows good agreement.

1. Introduction

The organic superconductors all have in common organic donor molecules derived from tetrathiafulvalene (denoted as TTF), tetraselenafulvalene (denoted at TSeF), or some mixture of these two molecules, packed into quasi one- and two-dimensional arrays and complexed to appropriate electron acceptors.[1] Figure 1 shows BEDT-TTF (denoted also as ET) which is the donor of the best organic superconductors. About 30 organic superconductors based on ET have been synthesized with T_c up to 12.8 K. Changes in T_c for various isotope shifts indicate that electron−phonon coupling is important for the superconductivity of these materials. However, experimental data on the vibrational modes is incomplete and does not supply clear evidence about which vibrational modes are important for the superconductivity. Consequently, we carried out ab initio Hartree−Fock (HF) and force field (FF) calculations to obtain all modes of neutral ET and of ET$^+$.

With appropriate electron acceptors some modifications of ET show superconductivity and some do not. The relation between superconductivity and the molecular or crystal structures of these molecules has not yet been clearly identified by the experiments. In this paper, we present calculated vibrational levels for the equilibrium structures of ET (boat) and ET$^+$ (planar). Using the calculated structures and Hessians with available experimental frequencies, we develop the MSX force fields for the neutral and cation ET molecules. These frequencies compare well with the available experimental frequencies[9,10] and provide procedures for a number of unknown or uncertain levels.

2. Results

2.1. Structures. The structure of ET is often discussed in terms of D_2 symmetry, which assumes a planar structure for the central TTF moiety. The crystal structures of neutral ET crystal are consistent with planarity but show a distinct boatlike distortion.[11] Some deviations from planarity are also suggested in crystals containing electron acceptors, $(ET)_nX_m$.[12] Here the ET molecules often form dimers $(ET_2)^+$ sharing a single positive charge.

Recently we reported ab initio quantum chemical calculations [Hartree−Fock (HF) with 6-31G** basis set] for the structures of neutral and cation ET.[7,8] These results show that the TTF framework for *neutral ET is nonplanar* deforming to a boat conformation with a well depth of 0.654 kcal/mol. However, the TTF framework for the cation, ET$^+$, is planar.

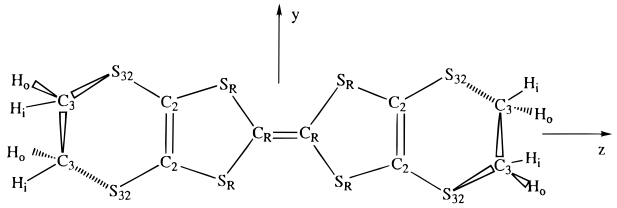

Figure 1. Definition of atomic types for the atoms of ET.

The terminal six-membered rings are nonplanar in order to avoid eclipsing of the CH_2-CH_2 groups at each end. This nonplanarity leads to two possible conformations:[12]

1. The *staggered* conformation indicated in Figure 1 in which the two C_6-C_6 bonds are pointing in opposite directions; assuming a planar TTF central region, this leads to D_2 symmetry.

2. The *eclipsed* conformation in which the two C_6-C_6 bonds are parallel; with planar TTF, this leads to C_{2h} symmetry. These conformations are essentially degenerate, differing by only 0.000 052 hartrees = 0.000 14 eV = 0.0032 kcal/mol (with eclipsed lower). We will consider hereafter the higher symmetry staggered case.

To determine the structure and vibrational modes of ET, we carried out ab initio Hartree−Fock calculations using the 6-31G** basis set.[13] Restricting the symmetry to D_2 leads to an optimized structure with two imaginary frequency vibrational modes. The stable conformation is the boat structure with C_2 symmetry (The optimized boat structure has vibration frequencies positive, indicating a stable structure).

2.2. Vibrational Analysis. Previous assignments of the vibrational spectra of ET have assumed planar molecule for both the neutral and cation cases. Planar ET would have D_2 symmetry for the staggered conformation and C_{2h} for the eclipsed conformation. For the staggered conformation this leads to fundamental modes with the following symmetries:

$$\Gamma(D_2) = 19A + 17B_1 + 18B_2 + 18B_3 \qquad (1)$$

To simplify assignments, Kozlov et al.[11,12] considered the ET to be totally flat leading to D_{2h} symmetries (they were aware

* To whom correspondence should be addressed.

[⊗] Abstract published in *Advance ACS Abstracts,* February 15, 1997.

S1089-5639(96)03004-6 CCC: $14.00 © 1997 American Chemical Society

TABLE 1: (A) Optimized Distances (in Å) for Boat and Planar ET Conformations and Experimental Distance (See Figure 1 for Notation) and (B) Optimized Angles (in deg)

A. Optimized Distances

		ET		ET^+	
		MSX[a]	HF	MSX	HF
C_R-C_R	1	1.325	1.326	1.389	1.389
S_R-C_2	4	1.773	1.774	1.751	1.751
$S_{32}-C_3$	4	1.812	1.814	1.816	1.816
S_R-C_R	4	1.769	1.771	1.721	1.721
C_2-C_2	2	1.325	1.323	1.336	1.336
$S_{32}-C_2$	4	1.769	1.767	1.765	1.765
C_3-C_3	2	1.523	1.523	1.523	1.523
C_3-H	8	1.083	1.082	1.082	1.082

B. Optimized Angles

		ET		ET^+	
		MSX	HF	MSX	HF
$S_{32}-C_2-C_2$	4	128.68	128.45	128.83	128.83
$S_R-C_2-S_{32}$	4	113.80	114.29	114.75	114.75
$S_R-C_R-S_R$	2	112.74	112.55	114.49	114.49
$C_R-S_R-C_2$	4	94.41	94.55	96.33	96.33
$S_{32}-C_3-C_3$	4	112.87	113.17	113.10	113.10
$S_R-C_2-C_2$	4	117.22	117.22	116.42	116.42
$S_R-C_R-C_R$	4	123.63	123.71	122.76	122.76
$C_2-S_{32}-C_3$	4	100.74	100.81	100.50	100.50
$H-C_3-H$	4	108.58	108.48	108.51	108.51
$S_{32}-C_3-H$	8	107.18	107.15	106.84	106.84
C_3-C_3-H	8	110.36	110.31	110.60	110.60

[a] For the neutral molecule, the optimized HF structure is minimized to reduce the total force by using FF. The rms force is less than 0.1 (kcal/mol)/Å for ET and ET^+.

that only the central C_2S_4 group is planar). This leads to the fundamental mode distribution

$$\Gamma(D_{2h}) = 12A_g + 7A_u + 6B_{1g} + 11B_{1u} + 7B_{2g} + 11B_{2u} + 11B_{3g} + 7B_{3u} \quad (2)$$

Thus D_{2h} leads to g and u branching of the D_2 symmetry modes. However, the stable boat structure of ET has C_2 symmetry, leading to the mode distribution

$$\Gamma(C_2) = 37A + 35B \quad (3)$$

Consequently, some modes become both infrared and Raman active. Table 4 shows that this is consistent with data of Kozlov et al.[9] The twofold axis of B_3 symmetry of the planar molecule and C_2 axis of the boat molecule are perpendicular to the central plane of the molecule. The reduction of symmetry is as follows:

$$12A_g + 7A_u + 11B_{3g} + 7B_{3u} \rightarrow 19A + 18B_3 \rightarrow 37A \quad (4a)$$

and

$$11B_{1u} + 6B_{1g} + 11B_{2u} + 7B_{2g} \rightarrow 17B_1 + 18B_2 \rightarrow 35B \quad (4b)$$

Table 4 shows all calculated frequencies plus available experimental frequencies for neutral ET. Calculated Raman and IR intensities are also given for all the vibrational modes. We used the symmetry of the modes for assigning experimental frequencies to the HF modes. The calculated IR and Raman intensities are in good agreement with experimental intensities.

ET^+ molecules in planar (D_2 symmetry), leading to the distribution of fundamental mode in eq 1. Table 5 shows all the vibrational modes of ET^+ compared to the available experimental frequencies.

3. The Force Field

The ET molecules appear to be distorted in the crystal structures, removing all symmetry. The assignment of frequencies for ET and ET^+ molecules by Kozlov et al.[9,10] assumed D_{2h} symmetry. We used the optimized HF geometries of the neutral and cation ET to develop the force fields. Neutral ET has C_2 symmetry and cation ET has D_2 symmetry. The optimized geometric parameters (distances, angles, dihedrals) for the neutral and cation ET molecules are given in Table 1. These structures are used in optimizing the force field (FF). (For the neutral molecule, the optimized HF structure is minimized to reduce the total force by using FF. The rms difference between HF and minimized structure (FF) are 0.002 Å for bonds, 0.680° for angles). We calculated the Hessian (second derivative of energy with respect to the 3N coordinates) at the HF optimized geometry. This Hessian was used to develop the force field by using Hessian-biased (HBFF) approach.[14]

The potential energy of the molecule is

$$E = \sum_{\text{bonds}} E_b + \sum_{\text{angles}} E_a + \sum_{\text{torsions}} E_t + \sum_{\text{inversions}} E_i + \sum_{\text{cross}} E_X + \sum_{\text{vdW}} E_{\text{vdW}} + \sum_{\text{charges}} E_Q \quad (5)$$

where the terms are defined below. This type of FF is denoted MSX to indicate that it is optimized for materials simulations and contains limited cross terms. Very often in fitting a FF to vibrational spectra, only valence force terms are used. We also include vdW and electrostatic parameters because we want to use the FF to predict the structures in crystal, where nonbonded interactions are critical.

In the HBFF approach, the potential energy is expressed as a sum of valence, nonbonded interactions. We optimize the force field terms by fitting the experimental frequencies and the calculated geometries.

3.1. Valence Interactions. We used the following valence terms:

(i) the harmonic bond stretch

$$E_b(R) = {}^1/_2 k_b (R - R_b)^2 \quad (6)$$

where R_b is the equilibrium bond distance and k_b is the force constant.

(ii) the harmonic angle bend

$$E_a(\theta) = {}^1/_2 k_\theta (\theta - \theta_0)^2 \quad (7)$$

where θ_0 is the equilibrium angle and k_θ is the force constant.

(iii) angle-stretch cross terms

$$E_{ab} = k_{R\theta}(\theta - \theta_0)(R - R_b) \quad (8)$$

where $k_{R\theta}$ is the force constant.

(iv) stretch−stretch cross terms

$$E_{bb} = k_{RR'}(R - R_b)(R' - R'_b) \quad (9)$$

where $k_{RR'}$ is the force constant for the bonds R_b and R'_b that share a common atom.

(v) the torsional potential

$$E_t(\phi) = V_0 + V_1 \cos\phi + V_2 \cos 2\phi + V_3 \cos 3\phi \quad (10)$$

where V_i is in kcal/mol and the angle ϕ is defined as the angle between the JKL plane and the IJK plane of the way two bonds IJ and KL attached to a common bond JK.

(vi) the inversion potential

$$E_i(\omega) = K_\omega(1 - \cos\omega) \tag{11}$$

with a minimum for planar structure ($\phi_0 = 0°$). ω is the angle between the *IL* axis and the *IJK* plane for an atom I with exactly three bonds *IJ*, *IK*, and *IL*.

3.2. Charges. Partial atomic charges for the various atoms were obtained using the potential derived charge method (PDQ).[15] The electron density from Hartree−Fock wavefunction is used to calculate the electrostatic potential around the molecule. Then, a set of atomic point charges is obtained that reproduces the ab initio electrostatic potential and dipole and quadrupole moments. Table 2 shows the atomic charges for the neutral and cation molecules.

We write total electrostatic energy as

$$E_{\text{Coulomb}} = C_0 \sum_{ij} \frac{Q_i Q_j}{\epsilon R_{ij}} \tag{12}$$

where ϵ is the dielectric constant, R_{ij} is the distance in Å, and the conversion factor $C_0 = 332.0637$ puts the energy in kcal/mol. We take $\epsilon = 1$ (i.e., vacuum).

3.3. van der Waals Parameters. We used the van der Waals parameters[16] previously determined from empirical fits to lattice parameters. The exponential-6 potential is used for van der Waals interactions:

$$E_{\text{vdW}} = D_{\text{v}}\left[\left(\frac{6}{\zeta - 6}\right) e^{\zeta(1-(R/R_{\text{v}}))} - \left(\frac{\zeta}{\zeta - 6}\right)\left(\frac{R_{\text{v}}}{R}\right)^6\right] \tag{13}$$

Table 3 gives the bond strength (well depth) D_{v} (in kcal/mol) and the bond length R_{v} (in Å) and ζ are given for C, S, and H.

The electrostatic and van der Waals interactions are excluded for 1−2, 1−3, and 1−4 interactions since they are considered to be already included in the bond stretch, angle bend, and torsion terms.

4. Hessian-Biased Method[14]

The potential energy is expanded around the equilibrium geometry.

$$E = E_0 + \sum_{i=1}^{3N}\left(\frac{\partial E}{\partial R_i}\right)(\delta R_i) + \frac{1}{2}\sum_{i,j=1}^{3N}\left(\frac{\partial^2 E}{\partial R_i\,\partial R_j}\right)(\delta R_i)(\delta R_j) + \ldots \tag{14}$$

where

$$F_i = -(\partial E/\partial R_i) \tag{15}$$

is the force on the *i*th component and

$$H_{ij} = \partial^2 E/\partial R_i\,\partial R_j \tag{16a}$$

is the Hessian. Using the mass weighting

$$\bar{H}_{ij} = H_{ij}(M_i M_j)^{-1/2} \tag{16b}$$

and diagonalizing (16b) leads to

$$\bar{H}\mathbf{U} = \mathbf{U}\lambda \tag{17}$$

where diagonal λ contains the $3N$ vibrational frequencies

$$\lambda_i = (108.5913\nu_i)^2$$

TABLE 2: Calculated Charges by Using Potential Derived Charge Method[15] (See Figure 1 for Notation)

	no. of cases	neutral	cation
C_R	2	−0.0200	−0.0220
S_R	4	−0.0260	0.1390
C_2	4	0.0265	0.0240
S_{32}	4	−0.0955	−0.0230
C_3	4	−0.1770	−0.2420
H_i	4	0.1885	0.2440
H_o	4	0.0935	0.1200
net charge		0.0	1.0

six of which have $\lambda_i = 0$ (here 108.5913 converts units so that energies are in kcal/mol, distances in Å, masses in amu, and ν_i in cm^{-1}).

In the Hessian-biased method, the theoretical Hessian (H_{t}) is biased with the experimental frequencies. From (17) the theoretical Hessian can be written

$$\bar{H}_{\text{t}} = \mathbf{U}_{\text{t}}\lambda_{\text{t}}\mathbf{U}_{\text{t}}^{\text{T}} \tag{18}$$

where $\mathbf{U}_{\text{t}}^{\text{T}}$ is the transpose of $\mathbf{U}_{\text{t}}$. We then replace λ_{t} with the experimental value λ_{x}. This leads to the *experimental biased Hessian* defined as

$$\bar{H}_{\text{xt}} = \mathbf{U}_{\text{t}}\lambda_{\text{x}}\mathbf{U}_{\text{t}}^{\text{T}} \tag{19a}$$

The biased Hessian has the property that

$$\bar{H}_{\text{xt}}\mathbf{U}_{\text{t}} = \mathbf{U}_{\text{t}}\lambda_{\text{x}} \tag{19b}$$

That is, it leads to the theoretical modes ($\mathbf{U}_{\text{t}}$) and the experimental frequencies (λ_{x}). If the λ_{x} is not available from experiment, it can be approximated from the theory by using appropriate scaling rules.

We optimized the force field parameters to obtain the best fit to $\bar{H}_{\text{xt}}$ while leading to correct (theoretical) equilibrium geometry. The van der Waals parameters and charges were fixed during optimization of the valence parameters. The charges (Table 2) were based on potential derived charges (PDQ) by using quantum mechanical potentials and the vdW parameters (Table 3) were from previous fits to various crystals.[16] The final force field parameters for the neutral and cation ET are shown in the first two columns of Table 3.

Calculated frequencies for ET and ET^+ are compared with the available experimental frequencies (Kozlov et al.[9,10]) in Tables 4 and 5. The average absolute error between theory and experiment is ∼13 cm^{-1} for ET and ∼16 cm^{-1} for ET^+. Applying the MSX force field to planar neutral BEDT-TTF (D_2 symmetry) led to two imaginary frequencies, which is consistent with the quantum mechanical results.[8]

5. Discussion

The best organic superconductors involve ET molecules. Isotopic shift experiments show that the mechanism for superconductivity in these materials must involve electron−phonon interactions.[8] In order to understand the mechanism of the superconductivity in these materials, we need to know the character of the phonon modes for the molecular crystals containing ET molecules. This requires a full characterization of the structures and vibrations of ET and ET^+. To provide this characterization, we performed quantum mechanical calculations determining the optimum structures for ET and ET^+. These results clarified the stable conformations of ET molecules and their symmetries and give vibrational frequencies (Table 4) consistent with the experiment. On the basis of the quantum mechanical results, we obtained MSX force field which accurately describes the vibrational spectrum. This force field

TABLE 3: Force-Field Parameters Used in This Calculation[a]

		vdW params[16]				vdW params[16]	
H	R_0	3.19500		S	ζ	14.03400	
	D_0	0.01520			R_0	4.03000	
	ζ	12.38200			D_0	0.34400	
C	R_0	3.89830			ζ	12.00000	
	D_0	0.09510					
bond stretch		neutral	cation	bond stretch		neutral	cation
C_3-H	R_b	1.084	1.081	$S_{32}-C_3$	R_b	1.821	1.825
	k_b	636.386	636.530		k_b	312.535	304.720
C_3-C_3	R_b	1.526	1.523	$S_{32}-C_2$	R_b	1.827	1.766
	k_b	613.257	606.042		k_b	361.172	479.499
C_2-C_2	R_b	1.300	1.329	S_R-C_2	R_b	1.788	1.753
	k_b	1280.633	1073.148		k_b	836.525	674.396
C_R-C_R	R_b	1.319	1.399	S_R-C_R	R_b	1.736	1.721
	k_b	1120.168	995.272		k_b	483.850	547.649
angle bend		neutral	cation	angle bend		neutral	cation
$H-C_3-H$	θ_0	109.12	108.65		k_θ	130.018	233.544
	k_θ	92.818	72.886	$S_R-C_2-S_{32}$	θ_0	108.09	114.96
C_3-C_3-H	θ_0	110.79	110.38		k_θ	89.224	90.533
	k_θ	80.057	109.365	$S_R-C_R-C_R$	θ_0	130.18	121.61
$S_{32}-C_3-H$	θ_0	107.44	105.85		k_θ	98.621	129.464
	k_θ	74.392	60.653	$S_R-C_R-S_R$	θ_0	128.78	116.13
$S_{32}-C_3-C_3$	θ_0	114.35	113.57		k_θ	154.837	148.992
	k_θ	193.274	364.201	$C_2-S_{32}-C_3$	θ_0	100.03	100.67
$S_{32}-C_2-C_2$	θ_0	121.64	127.48		k_0	198.691	191.985
	k_θ	96.121	77.349	$C_R-S_R-C_2$	θ_0	98.32	96.85
$S_R-C_2-C_2$	θ_0	113.62	115.72		k_θ	250.173	322.658
angle cross terms		neutral	cation	angle cross terms		neutral	cation
$H-C_3-H$	$k_{R_1\theta}$	−75.260	−27.305		$k_{R_1R_2}$	408.025	264.133
	$k_{R_2\theta}$	−75.260	−27.305	$S_R-C_2-S_{32}$	$k_{R_1\theta}$	54.907	35.455
	$k_{R_1R_2}$	−38.305	−22.977		$k_{R_2\theta}$	113.414	135.257
C_3-C_3-H	$k_{R_1\theta}$	7.847	6.245		$k_{R_1R_2}$	86.875	91.696
	$k_{R_2\theta}$	3.295	86.784	$S_R-C_R-C_R$	$k_{R_1\theta}$	40.592	69.328
	$k_{R_1R_2}$	1.546	−0.226		$k_{R_2\theta}$	36.508	104.725
$S_{32}-C_3-H$	$k_{R_1\theta}$	48.635	39.139		$k_{R_1R_2}$	63.775	29.613
	$k_{R_2\theta}$	18.933	−10.670	$S_R-C_R-S_R$	$k_{R_1\theta}$	79.702	126.993
	$k_{R_1R_2}$	−13.325	−0.371		$k_{R_2\theta}$	79.702	126.993
$S_{32}-C_3-C_3$	$k_{R_1\theta}$	−0.964	−6.689		$k_{R_1R_2}$	60.025	19.556
	$k_{R_2\theta}$	−4.778	68.070	$C_2-C_{32}-C_3$	$k_{R_1\theta}$	49.887	148.984
	$k_{R_1R_2}$	20.436	34.745		$k_{R_2\theta}$	46.465	33.800
$S_{32}-C_2-C_2$	$k_{R_1\theta}$	96.007	119.264		$k_{R_1R_2}$	−11.975	−69.191
	$k_{R_2\theta}$	−47.517	−31.109	$C_R-S_R-C_2$	$k_{R_1\theta}$	52.029	124.512
	$k_{R_1R_2}$	10.424	−2.801		$k_{R_2\theta}$	59.718	43.796
$S_R-C_2-C_2$	$k_{R_1\theta}$	178.792	162.888		$k_{R_1R_2}$	10.704	25.593
	$k_{R_2\theta}$	81.403	82.593				
torsion terms		neutral	cation	torsion terms		neutral	cation
$H-C_3-C_3-H$	V_3	5.958	7.164	$C_3-C_{32}-C_2-S_R$	V_2	−0.020	0.170
$S_{32}-C_3-C_3-H$	V_3	19.558	9.641	$C_R-S_R-C_2-C_2$	V_2	2.764	−3.149
$S_{32}-C_3-C_3-S_{32}$	V_3	−73.125	−57.046	$C_R-S_R-C_2-S_{32}$	V_2	−0.774	−4.459
$S_{32}-C_2-C_2-S_{32}$	V_2	−25.759	−3.196		V_3	1.845	0.000
$S_R-C_2-C_2-S_{32}$	V_2	10.814	−13.975	$C_2S_R-C_R-C_R$	V_1	6.756	12.840
$S_R-C_2-C_2-S_R$	V_2	−44.726	0.876		V_2	0.844	0.263
$S_R-C_R-C_R-S_R$	V_2	−19.943	−0.217		V_3	−0.350	0.000
$C_2-S_{32}-C_3-H$	V_3	1.531	0.684	$C_2-S_R-C_R-S_R$	V_2	1.175	−1.393
$C_2-S_{32}-C_3-C_3$	V_3	−2.586	−2.605		V_3	2.127	0.000
$C_3-S_{32}-C_2-C_2$	V_2	0.720	1.825				
inversion constant (K_ω)		neutral	cation	inversion constant (K_ω)		neutral	cation
$C_2-S_R-S_{32}-C_2$		5.738	4.917	$C_R-S_R-S_R-C_R$		10.713	16.128
$C_2-S_R-C_2-S_{32}$		85.778	155.854	$C_R-S_R-C_R-S_R$		53.616	50.178
$C_2-S_{32}-C_2-S_R$		6.745	1.651				

[a] Units are kcal/mol for energies, Å for length, and degrees for angles. Angular force constants use radians.

can be used in molecular dynamic simulations for crystals containing ET and ET^+. This should be useful in explaining the superconductivity of these systems.

We find that some vibrational modes of staggered ET molecule (C_2 symmetry) allow both IR and Raman activities. This allows the electrons coupling several vibrational modes which would be forbidden for planar donor molecules which are more symmetric (D_2 symmetry). This may be important in the superconducting properties.

6. Summary

We developed the MSX force fields for the neutral and cation ET molecules including both valence and nonbonded interactions. The Hessian-biased approach is used to obtain a force

TABLE 4: Calculated (HF) and Experimental Frequencies and Raman and Infrared (IR) Intensities for ET[a]

		HF						
			intensity		experiment			
sym	modes	ν_i	IR	Raman	IR	Raman	MSX	error
A	C−H str	3302	11.60	71.75			2957.9	
B	C−H str	3302	3.28	51.36	2958 w[b]		2957.9	0
A	C−H str	3290	0.01	256.30			2915.0	
B	C−H str	3290	0.37	9.60			2915.0	
A	C−H str	3237	0.20	606.22			2958.3	
B	C−H str	3237	79.71	4.30	2958 w		2958.3	0
A	C−H str	3229	10.24	161.39			2909.8	
B	C−H str	3228	2.68	6.80		2916 w	2909.8	6
A	C═C str	1815	0.57	354.11		1552 m	1546.9	5
B	C═C str	1790	1.48	0.26	1505 w	*1511 m*	1519.5	9
A	C═C str	1772	0.35	509.60		1494 s	1490.0	4
A	CH_2 bend	1608	3.02	10.70			1424.3	
B	CH_2 bend	1608	1.11	14.73	1420 w		1424.3	4
A	CH_2 bend	1594	11.27	9.51		1406 m	1401.4	5
B	CH_2 bend	1594	4.86	32.12	1409 vw		1401.4	8
A	CH_2 wag	1466	2.41	0.93		1285 vw	1295.0	10
B	CH_2 wag	1466	63.72	1.71	1282 m		1295.0	13
A	CH_2 wag	1434	5.66	1.19	1259 w		1247.4	12
B	CH_2 wag	1434	0.90	0.57	1253 vw	*1256 vw*	1247.4	9
A	CH_2 twist	1321	0.27	15.70			1164.2	
B	CH_2 twist	1321	0.06	2.33	1173 vw	*1175 vw*	1164.2	11
A	CH_2 twist	1260	2.48	0.29	1132 sh	*1132 vw*	1127.4	5
B	CH_2 twist	1260	2.44	14.41	*1125 w*	1126 vw	1127.4	2
A	ring def (IP)[c]	1131	0.21	0.34		1016 vw	1029.5	13
B	ring def (IP)	1128	7.06	0.02			1013.0	
A	ring def (IP)	1125	0.01	0.59			1009.3	
B	C−C str	1093	0.03	0.61	*996 w*	1002 w	998.6	3
A	C−C str	1093	0.01	7.15	987 w	*990 w*	998.6	9
A	CH_2 rock	1033	1.64	7.62			948.1	
B	CH_2 rock	1033	22.58	5.39	938 vw		948.1	10
B	CH_2 wag	996	12.99	1.83	917 s		915.5	1
A	CH_2 wag	990	5.72	0.04		919 vw	915.5	3
B	ring def (IP)	967	28.10	0.77	905 m		900.0	5
A	ring def (IP)	967	3.50	1.81		911 vw	899.6	11
B	ring def (IP)	951	2.29	0.28	*890 m*	888 vw	854.1	36
B*	ring def (IP)	847	12.03	0.13	875 vw	*875 w*	758.6	16
B	ring def (IP)	846	42.37	0.02	*772 s*	765 w	761.6	10
A	ring def (IP)	842	0.17	1.96	860 vw	*860 vw*	824.4	36
A	CH_2 rock	759	0.10	15.90		687 w	726.8	40
B	CH_2 rock	759	2.47	1.86	687 w		724.9	38
A	CH_2 rock	716	0.02	44.08		653 m	629.9	23
B	CH_2 rock	716	6.70	0.62	653 w		628.9	24
B	ring def (OP)[d]	623	4.54	11.88			724.9	
B	ring def (OP)	606	0.06	4.15			453.3	
A	ring def (OP)	605	0.05	0.92			449.6	
A	ring def (OP)	539	1.50	15.60		486 m	502.3	16
B	ring def (IP)	511	1.50	0.86	499 m		481.3	18
A	ring def (IP)	510	0.03	1.73		625 w	668.6	44
B	ring def (IP)	496	6.24	0.43	624 w		667.8	44
A	ring def (IP)	483	0.01	14.54	450 w	*440 m*	446.0	6
B	ring def (IP)	425	6.63	1.16	390 m		389.3	1
B	ring def (IP)	394	0.04	0.80		334 m	361.6	28
A	ring def (IP)	393	0.02	0.10	335 m		373.4	38
A	ring def (IP)	383	0.09	8.42		348 w	347.3	1
A	ring def (OP)	356	1.02	4.00		308 w	303.0	5
B	ring def (OP)	327	3.16	0.17	*278 m*	272 vw	288.1	10
A	ring def (OP)	315	0.04	2.72			361.9	
B	ring def (OP)	309	0.28	0.05			269.8	
A	ring def (OP)	300	0.04	0.20			261.4	
B	ring def (IP)	286	3.72	0.02	*257 m*	260 w	264.9	8
A	ring def (OP)	270	0.01	0.75			177.1	
B	ring def (OP)	262	4.45	0.61			177.0	
A	ring def (OP)	206	0.01	0.72		159 s	183.5	25
A	ring def (IP)	173	0.03	14.86		151 s	153.6	3
A	ring def (OP)	130	0.03	0.18		127 vw	127.0	0
B	ring def (OP)	129	0.00	0.28			62.2	
B	ring def (IP)	60	1.14	0.87	96 m		98.1	2
A	ring def (OP)	53	0.16	0.19			53.1	
B	ring def (OP)	44	2.71	0.37			46.7	
A	ring def (OP)	42	7.24	0.26			45.2	
B	ring def (OP)	38	0.26	0.63	*30 w*	31 vs	36.9	7
A	ring def (OP)	20	2.21	1.28			15.7	
av abs error		109						13

[a] The frequencies are in cm^{-1}, IR intensities are in km/mol (1 km/mol = 0.0236 66 D^2 $Å^{-2}$ amu^{-1}), Raman intensities are in $Å^4$/amu. We used the italic ones (the assignments of Kozlov[9]) for the error calculations for the modes which appears both in IR and Raman spectra. [b] Relative intensities: vs, very strong; s, strong; m, medium; w, weak; vw, very wak; sh, shoulder; br, broad. [c] In-plane ring deformation mode. [d] Out-of-plane ring deformation mode.

TABLE 5: Calculated and Experimental Frequencies and Raman and Infrared (IR) Intensities for ET^{+a}

		HF						
			intensity		experiment			
sym	modes	ν_i	IR	Raman	IR	Raman	MSX	error
B_3	C−H str	3316	1.41	90.73	2936 w[b]		2935.9	0
B_2	C−H str	3316	0.21	86.51			2935.9	
A	C−H str	3305	0.00	251.75			2916.5	
B_1	C−H str	3305	2.13	0.57	2914 vw		2916.5	2
A	C−H str	3248	0.00	1086.34			2871.1	
B_1	C−H str	3248	24.15	1.76		2847 vw ?	2871.1	
B_2	C−H str	3242	0.29	13.57	2883 w		2857.5	25
B_3	C−H str	3242	5.22	179.42			2857.5	
A	C═C str	1697	0.00	60707.55		1455 m	1496.0	41
B_1	C═C str	1620	3060.40	1.32	1445 w		1457.7	13
A	CH_2 bend	1601	0.00	24.83			1422.2	
B_1	CH_2 bend	1601	5.04	4.97	1422 sh		1422.2	0
B_3	CH_2 bend	1594	23.93	6.92	1411 s		1416.4	5
B_2	CH_2 bend	1594	4.55	56.09			1416.4	
A	C═C str	1565	0.00	34573.66		1431 vs	1385.1	46
A	CH_2 wag	1469	0.00	279.93		1294 vw	1285.5	8
B_1	CH_2 wag	1467	209.74	1.47	1283 m		1485.3	2
B_3	CH_2 wag	1435	7.32	3.71		1274 vw	1263.6	10
B_2	CH_2 wag	1435	0.00	0.72	1277 sh		1263.6	13
A	CH_2 twist	1325	0.00	16.62			1173.5	
B_1	CH_2 twist	1325	1.47	2.08	1180 w ?		1173.5	
B_3	CH_2 twist	1264	1.38	1.56	1125 sh ?		1135.0	
B_2	CH_2 twist	1264	2.21	18.511		1120 w	1135.0	15
B_3	ring def (IP)[c]	1171	0.25	623.99		1056 w	1059.4	3
B_2	ring def (IP)	1141	16.86	0.06	1024 w		1026.3	2
B_3	ring def (IP)	1138	0.10	5.88			1025.6	
A	C−C str.	1093	0.00	31.22		976 mw	991.2	15
B_1	C−C str	1093	0.30	0.61	1010 vw		991.2	19
A	CH_2 rock	1029	0.00	247.37		931 vw ?	952.3	
B_1	CH_2 rock	1029	5.24	5.10			936.4	
B_2	CH_2 wag	997	0.04	2.42	915 w		935.7	21
B_3	CH_2 wag	991	8.04	0.00			887.1	
B_2	ring def (IP)	969	4.06	74.29	900 w		895.7	4
A	ring def (IP)	963	0.00	7905.13		905 w	885.0	20
B_1	ring def (IP)	927	5.84	225.12			950.9	
B_1	ring def (IP)	881	5.86	956.10	812 w		826.0	14
B_2	ring def (IP)	857	6.11	0.09	886 w,br		841.1	45
B_3	ring def (IP)	853	0.29	3.72			839.3	
B_3	CH_2 rock	749	0.00	13.32			691.6	
B_2	CH_2 rock	749	4.23	2.77	640 vw		691.6	52
A	CH_2 rock	707	0.00	339.78			686.4	
B_1	CH_2 rock	706	36.60	0.04	672 vw		684.9	13
B_1	ring def (OP)[d]	610	0.01	3.23			636.0	
A_2	ring def (OP)	607	0.00	14.03			636.0	
B_2	ring def (OP)	596	0.02	6.19			581.2	
A	ring def (IP)	570	0.00	5148.20		511 mw	512.9	2
B_3	ring def (IP)	514	0.35	0.04			487.1	
B_2	ring def (IP)	512	2.91	1.11			476.5	
B_1	ring def (IP)	504	605.79	0.00	503 w		512.0	9
A	ring def (IP)	492	0.00	2986.58		489 m	453.9	35
B_1	ring def (IP)	438	3.85	0.05	406 w		397.6	8
B_2	ring def (IP)	392	0.49	0.2			344.6	
B_3	ring def (IP)	387	0.06	4.84	357 vw	*355 vw*	387.0	32
B_3	ring def (IP)	371	0.00	93.14	335 w		349.14	14
B_3	ring def (OP)	357	1.70	0.21			340.3	
A	ring def (IP)	348	0.00	4.39		320 w	335.2	15
B_1	ring def (IP)	328	21.53	0.04			339.7	
B_2	ring def (OP)	309	0.52	3.25	265 w		272.7	8
B_2	ring def (IP)	295	4.79	0.01			335.2	
B_3	ring def (OP)	294	0.07	0.32			282.2	
A	CH_2 wag	294	0.00	0.32			234.0	
B_1	CH_2 wag	283	0.00	0.07			219.5	
B_3	ring def (IP)	187	0.01	3.46			179.8	
A	ring def (IP)	175	0.00	185.20		169 w	162.8	6
A	ring def (OP)	120	0.00	6.81			83.6	
B_1	ring def (OP)	120	0.48	0.57			83.1	
B_2	ring def (OP)	86	0.07	16.63			70.3	
B_2	ring def (IP)	61	0.16	0.00			53.6	
B_3	ring def (OP)	49	8.93	0.29			46.1	
B_2	ring def (OP)	43	0.02	0.17			34.4	
A	ring def (OP)	36	0.00	0.00			19.8	
B_3	ring def (OP)	28	2.04	0.02			8.4	
av abs error		121						16

[a] The frequencies are in cm^{-1}, IR intensities are in km/mol (1 km/mol = 0.0236 66 D^2 $Å^{-2}$ amu^{-1}) 42.2547, Raman intensities are in $Å^4$/amu. We used the italic ones (the assignments of Kozlov[10]) for the error calculations for the modes which appears both in IR and Raman spectra. ?: These experimentally uncertain modes are not included in error calculations.[10] [b] Relative intensities: vs, very strong; s, strong; m, medium; w, weak; vw, very weak; sh, shoulder; br, broad. [c] In-plane ring deformation mode. [d] Out-of-plane ring deformation mode.

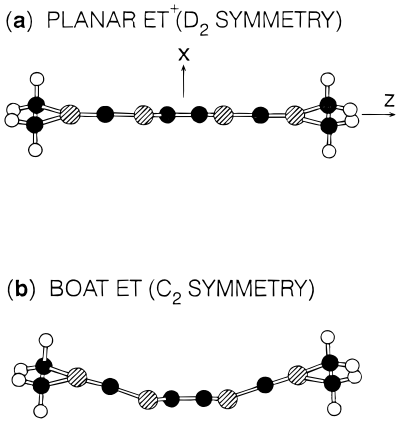

Figure 2. Side view for optimum structures (a) ET^+ and (b) ET. Here C is a solid circle, S is a cross-hatched circle, and H is an open circle.

field which reproduces experimental frequencies for the neutral and cation ET while retaining the correct structural and vibrational characteristics for the models. The calculated frequencies are in good agreement with the available experimental frequencies for the neutral and cation ET molecules. This should be useful in characterizing the superconductors.

Acknowledgment. This research was supported by the NSF (CHE 95-22179 and ASC 92-17368). The facilities of the MSC are also supported by grants from DOE-AICD. Chevron Petroleum Technology, Asahi Chemical, Chevron Chemical Co., Hercules, Avery Dennison, Chevron Refinery Technology, and the Beckman Institute. Some of these calculations were carried out at Pittsburgh NSF Supercomputer Center and on the JPL Cray computers.

References and Notes

(1) Jerome, D.; Mazaud, A.; Ribault, M.; Bechgaard, K. *J. Phys. Lett.* **1980**, *41*, L95.

(2) Yamaji, K. *Solid State Commun.* **1987**, *61*, 413.

(3) Carlson, K. D.; Williams, J. M.; Geiser, U.; Kini, A. M.; Wang, H. H.; Klemm, R. A.; Kumar, S. K.; Schlueter, J. A.; Ferraro, J. R.; Lykke, K. R.; Wurz, P.; Parker, H.; Sutin, J. D. B. *Mol. Crsyt. Liq. Cryst.* **1993**, *234*, 127.

(4) Carlson, K. D.; Kini, A. M.; Klemm, R. A.; Wang, H. H.; Williams, J. M.; Geiser, U.; Kumar, S. K.; Ferraro, J. R.; Lykke, K. R.; Wurz, P.; Fleshler, S.; Dudek, J. D.; Eastman, N. L.; Mobley, P. R.; Seaman, J. M.; Sutin, J. D. B.; Yaconi, G. A. *Inorg. Chem.* **1992**, *31*, 3346.

(5) Carlson, K. D.; Kini, A. M.; Schlueter, J. A.; Wang, H. H.; Sutin, J. D. B.; Williams, J. M.; Schirber, J. E.; Venturini, E. L.; Bayless, W. R. *Physica C* **1994**, *227*, 10.

(6) Carlson, K. D.; Williams, J. M.; Geiser, U.; Kini, A. M.; Wang, H. H.; Klemm, R. A.; Kumar, S. K.; Schlueter, J. A.; Ferraro, J. R.; Lyyke, K. R.; Wurz, P.; Parker, D. H.; Sutin, J. D. B. *Mol. Cryst. Liq. Cryst.* **1993**, *234*, 127.

(7) Demiralp, E.; Goddard, III, W. A. *Synth. Met.* **1995**, *72*, 297.

(8) Demiralp, E.; Dasgupta, S.; Goddard, W. A., III *J. Am. Chem. Soc.* **1995**, *117*, 8154.

(9) Kozlov, M. E.; Pokhodnia, K. I.; Yurchencko, A. A. *Spectrochim. Acta* **1989**, *45A*, 323.

(10) Kozlov, M. E.; Pokhodnia, K. I.; Yurchencko, A. A. *Spectrochim. Acta* **1989**, *45A*, 437.

(11) Kobayashi, H.; Kobayashi, A.; Yukiyoshi, S.; Saito, G.; Inkuchi, H. *Bull. Chem. Soc. Jpn.* **1986**, *59*, 301.

(12) Williams, J. M.; Ferraro, J. R.; Carlson, K. D.; Geiser, U.; Wang, H. H.; Kini, A. M.; Whangbo, M-H, *Organic Superconductors (Including Fullerenes): synthesis, structure, properties, and theory*; Prentice-Hall: New York, 1992.

(13) The quantum chemical calculations were carried out using: *Gaussian 92*, Revision B; Frisch, M. J.; Trucks, G. W.; Head-Gordon, M.; Gill, P. M. W.; Wong, M. W.; Foresman, J. B.; Johnson, B. G.; Schlegel, H. B.; Robb, M. A.; Replogle, E. S.; Gomperts, R.; Andres, J. L.; Raghavachari, K.; Binkley, J. S.; Gonzalez, C.; Martin, R. L.; Fox, D. J.; Defrees, D. J.; Baker, J.; Stewart, J. J. P.; Pople, J. A. Gaussian, Inc.: Pittsburgh, PA, 1992.

(14) Dasgupta, S.; Goddard, W. A., III *J. Phys. Chem.* **1989**, *95*, 7207.

(15) (a) Ringnalda, M. N.; Langlois, J-M.; Greeley, B. H.; Russo, T. V.; Muller, R. P.; Marten, B.; Won, Y.; Donnelly, Jr., R. E.; Pollard, W. T.; Miller, G. H.; Goddard, W. A., III; Freisner, R. A. PS-GVB v1.0, Schrödinger, Inc., Pasadena, CA, 1994. (b) Greeley, B. H.; Russo, T. V.; Mainz, D. T.; Friesner, R. A.; Langlois, J-M.; Goddard, W. A., III; Donnelly, R. E.; Ringnalda, M. N. *J. Chem. Phys.* **1996**, *101*, 4028.

(16) Mayo, S. L.; Olafson, B. D.; Goddard, W. A., III *J. Phys. Chem.* **1990**, *94*, 8897.

(17) Eldridge, J. E.; Homes, C. C.; Wang, H. H.; Kini, A. M.; Williams, J. M. *Synth. Met.* **1995**, *70*, 983.